Appl Phys B (2009) 96: 613–621
DOI 10.1007/s00340-009-3520-1

Applied Physics B
Lasers and Optics

The effects of pulsed laser injection seeding and triggering on the temporal behavior and magnitude of laser-induced incandescence from soot

F. Goulay · P.E. Schrader · H.A. Michelsen

Received: 9 January 2009 / Revised version: 6 March 2009 / Published online: 2 May 2009

Abstract The effect of sub-nanosecond fluence fluctuations and triggering on time-resolved laser-induced incandescence (LII) from soot has been studied using an injection-seeded pulsed Nd:YAG laser that produces a smooth laser temporal profile. Without injection seeding, this multi-mode laser generates pulses with large intensity fluctuations with sub-nanosecond rise times. The experimental results described here demonstrate that at fluences below 0.6 J/cm^2 LII signals are insensitive to fluence fluctuations on nanosecond time scales. At fluences above 0.6 J/cm^2 fluctuations in the laser profile cause the rising edge of the LII profile to move around in time relative to the center of the laser pulse causing a broader average profile that shifts to earlier times. Such fluctuations also lead to a decrease in the average LII temporal profile by up to 12% at a fluence of 3.5 J/cm^2. A timing jitter on the trigger of the data acquisition, such as that produced by triggering on the laser Q-switch synchronization pulse, has a negligible effect on the shape and temporal maximum of the LII signal. Additional jitter, however, considerably reduces the peak of the LII temporal profiles at fluences as low as 0.15 J/cm^2. Neither fast fluence fluctuations nor trigger jitter have a significant effect on gated LII signals, such as those used to infer soot volume fraction.

PACS 65.80.+n · 78.20.Nv · 42.62.-b

F. Goulay · P.E. Schrader · H.A. Michelsen (✉)
Combustion Research Facility, Sandia National Laboratories, P.O. Box 969, MS 9055, Livermore, CA 94551, USA
e-mail: hamiche@sandia.gov

1 Introduction

Laser-induced incandescence (LII) is frequently used as a sensitive optical technique for measurements of soot volume fraction and primary particle size [1]. In the implementation of LII, soot particles are heated with a high-power pulsed laser to temperatures (2500–4200 K) at which they incandesce, and the emitted light is collected and measured. Temporally resolved LII signals increase during the laser pulse, as particles undergo absorptive heating, and decrease after the laser pulse, as particles conductively and evaporatively cool.

The magnitude of the LII signal is nominally proportional to the soot volume fraction [1–4] whereas the signal decay rate, at low fluences and long collection times, depends on the soot conductive cooling rate and thus on the surface area to volume ratio. Soot volume fractions are generally measured by gating the LII signal collected over broad ranges of wavelength, and primary particle sizes are inferred from time-resolved signals at discrete wavelengths or in a wavelength region excluding C_2 Swan band emission [5–15]. Accurate quantitative measurements with LII are limited by an incomplete understanding of the physical mechanisms and measurement parameters that influence signal evolution during and after the laser pulse. Measurement parameters to which the LII signal has been shown to be sensitive include ambient temperature and pressure [8, 16–20], detection wavelength range [21, 22], laser beam spatial profile [4, 23–27] and its temporal evolution [28], laser pulse duration [29], gate width, gate delay [30–33], and laser fluence [22, 23, 25, 33–37].

Absorptive heating is a single-photon process and is linear with fluence, such that, at fluences below ∼0.09 J/cm^2, the maximum temperature the particles reach has a linear fluence dependence. At these low fluences conduction to

the surrounding atmosphere is the dominant cooling mechanism and leads to decay times on the order of a few hundred nanoseconds [12, 23, 25, 33, 34, 38]. At fluences above ~0.12 J/cm^2, particles begin to shrink and cool by sublimation [2, 5, 11, 12, 34, 38–41]. Decay times decrease with increasing fluence [11, 21, 23, 25, 33, 34, 40], and signals start to decay during the laser pulse. At even higher fluences sublimation limits the maximum temperature reached by the particles, and multi-photon processes may further affect the LII signal. Depending on the total fluence, the LII profiles can be sensitive to laser intensity fluctuations during the laser pulse.

LII measurements of soot are frequently made using a 1064- or 532-nm multi-mode laser to heat the particles. The single-pulse temporal profiles from these lasers can have large intensity fluctuations with sub-nanosecond rise times. In the present work we have investigated the influence of such fluctuations on the magnitude and temporal evolution of the LII signal. In order to study the effect of injection seeding on the LII temporal profile, we compare single-pulse and averaged LII temporal profiles with the injection seeder turned on and with the seeder turned off at fluences of 0.08, 0.6, and 3.0 J/cm^2. The effect of the injection seeding on the LII temporal maximum was studied by comparing averaged LII profiles for both laser modes at fluences ranging form 0.01 to 3.5 J/cm^2. At low fluences, because the LII response time is much longer than the characteristic time of the laser intensity fluctuations, the effect of injection seeding on the temporal profile and temporal maximum of the LII is minimal. At higher fluences the LII temporal profiles and maximum signal intensity depend on the shape of the pulse-to-pulse laser profile, likely because of fast (sub-nanosecond) nonlinear absorption processes that affect the particle temperature and size.

Moreover, at intermediate and high fluences the LII signal rise time decreases with increasing fluence and, at fluences above the sublimation threshold, signal decay rates increase. This combination of effects leads to a narrowing of the peak of the temporal profiles with increasing laser fluence. We have found that capturing this behavior requires the use of a detector with a fast (sub-nanosecond) time response. When multiple laser shots are averaged, recording the sharp peak of the LII signal also requires an optical trigger with a fast time response for data acquisition. Using a slower detector for the signal or relying on a trigger that introduces jitter relative to the laser pulse will lead to a measured slower averaged signal rise time and decay rate and a lower peak signal at intermediate and high fluences. LII data are often recorded using the laser Q-switch synchronization pulse (referred to as the Q-switch) to trigger the data acquisition. This triggering approach introduces jitter (typically on the order of 0.5–1 ns) relative to the laser pulse. In the present work we have investigated the effect on the LII signal of triggering on the Q-switch. With the injection seeder on, data were collected using the Q-switch and the laser flashlamp synchronization pulse modified to add jitter. Averaged LII temporal profiles were recorded over the entire experimental fluence range using the Q-switch and at selected fluences of 0.06, 0.15, 0.3, 0.6, 1.5, and 3.0 J/cm^2 when using the modified flashlamp pulse. Triggering on the Q-switch of our laser has a negligible effect on LII signals. Additional jitter, however, affects the shape and maximum intensity of average LII temporal profiles at fluences as low as 0.15 J/cm^2.

2 Experimental setup

A schematic diagram of the experimental setup is shown in Fig. 1. Soot is generated in a non-smoking laminar diffusion flame at atmospheric pressure. The burner with which it is produced, commonly known as a Santoro burner, has a brass fuel tube with a 1.1-cm inner diameter surrounded by ceramic honeycomb with a 10.2-cm outer diameter for the co-flow of air [23, 42–47]. The flame is stabilized with a chimney 19.5-cm tall and 10.2 cm in diameter. Mass-flow controllers (MKS types 1479A for low flow and 1559A for high flow) are used to maintain flow rates in the ranges of 0.23 standard liters per minute (slm) ethylene for the fuel and 42 slm for the air. These flow conditions have been used in previous work performed with the Santoro burner [44–46, 48]. The visible flame height is 9.8 cm. Measurements are made at a height of 5 cm above the burner on the edge of the flame closest to the laser to avoid laser attenuation in the flame and re-absorption of LII between the detection region in the flame and the detector.

An injection-seeded Nd:YAG laser (Spectra-Physics Pro-230-10 with a Spectra-Physics 6350-1 seeder) generates 532-nm pulses with a pulse duration of 8.3 ns FWHM and beam diameter of ~0.61 cm. A ceramic aperture with a diameter of 0.2 cm is placed at the output of the laser to select the central portion of the beam resulting in a temporal spread of less than 400 ps over the selected beam area [28]. The aperture is relay imaged to the detection region in the flame using a telescope with a 100-cm lens followed by a 50-cm lens, the combination of which produces a collimated beam approximately half the diameter of the aperture (0.1 cm). A beam profiler with a 6.7 × 6.7 μm^2 pixel size (DataRay WinCamD-UCM) is used to monitor the spatial profile produced at the flame by this optical configuration (see Fig. 1). The beam is attenuated with a half-wave plate followed by two thin-film polarizers, and the fluence is monitored using a surface-absorbing thermal detector (Molectron PM10). The beam profiles are independent of fluence.

The LII signal is imaged using a telescope with a magnification of four onto a fast amplified silicon photodiode

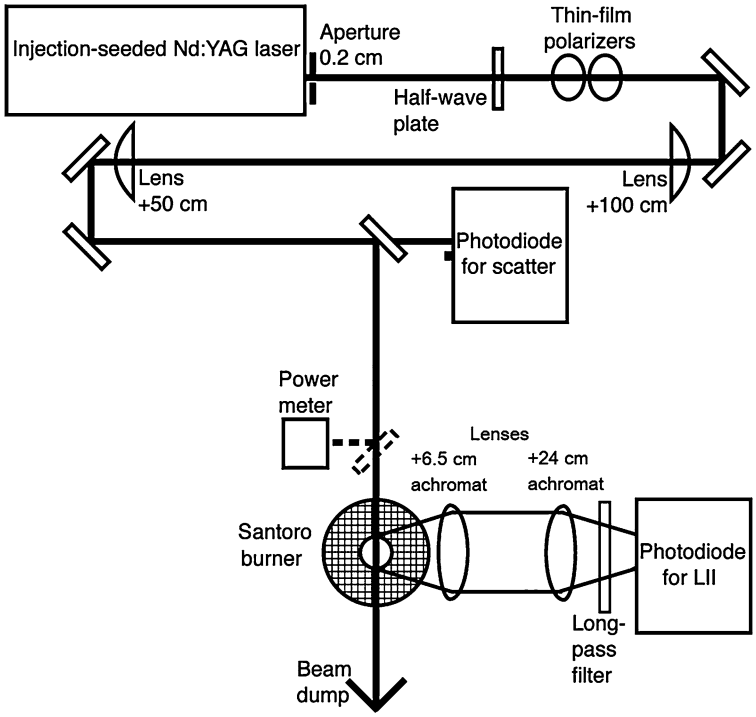

Fig. 1 Experimental setup

(Electro-Optics Technology ET-2030A) with a rise time of ∼200 ps and an active area of 0.04-cm diameter. A silicon photodiode (Electro-Optics Technology ET-4000) with a 35-ps rise time, viewing 532-nm light from the laser, is used to measure the laser temporal profile simultaneously with the LII measurements. Signals are recorded on an oscilloscope with a 3-GHz bandwidth (Tektronics TDS694C), which is triggered using (1) a fast InGaAs photodiode (Electro-Optics Technology ET-3500) viewing 1064-nm light leaking through the first dichroic mirror, i.e. prior to the half-wave plate used for attenuation, (2) the laser Q-switch, or (3) the flashlamp synchronization pulse modified using a low-pass electrical filter to increase the rise time of the leading edge of the pulse, thereby increasing the inherent timing jitter. LII temporal profiles are recorded at a temporal resolution of 10 GS/s at fluences between 0.02 and 3.5 J/cm^2. LII signals are collected using a 700-nm long wave pass filter (Newport 10LWF-700-B) in combination with a 532-nm holographic notch filter (Kaiser Optical System HNPF-532.0-1.0) to avoid collection of any non-LII light [22].

3 Results and discussion

3.1 Influence of injection seeding

Laser temporal profiles Figure 2 compares laser temporal profiles from the second harmonic of the pulsed Nd:YAG laser for (a) 300 single laser pulses and (b) the average of 300 laser pulses. The laser profiles were recorded with the injection seeder turned on (black lines) and with the seeder turned off (grey lines). All the laser profiles displayed in Fig. 2 have been normalized to the areas under the curves. Because of the mode structure of the unseeded laser pulses, deviations in the instantaneous intensity from a smooth (seeded) pulse can be as much as 60%. Most of the structure observed for the unseeded single-pulse temporal profiles is randomly timed such that the averaged temporal profiles from the unseeded laser, shown in Fig. 2b, are much smoother than the temporal profiles from individual pulses. When measuring the laser profile with a sub-nanosecond resolution, however, there is some residual structure in the 300-pulse-averaged unseeded-laser profile. Consequently, the averaged temporal profile is not as smooth as that of the seeded laser. The additional sharp features are separated by 5 ns, which corresponds to the 200-MHz frequency spacing between the laser cavity longitudinal modes. The remaining structure is therefore likely to be due to partial mode locking in the cavity and can be detected only when recording the laser pulse with a sub-nanosecond time resolution. The averaged (area-normalized) laser profiles for both laser modes displayed in Fig. 2b do not differ in instantaneous intensity by more than 20%.

LII temporal response Figure 3 displays single-pulse LII profiles recorded at a fluence of 0.6 J/cm^2 with the laser seeder turned on (Figs. 3a and b) and with the laser seeder turned off (Figs. 3c and d) using an optical trigger. For clarity only 20 single pulses are displayed. LII profiles recorded

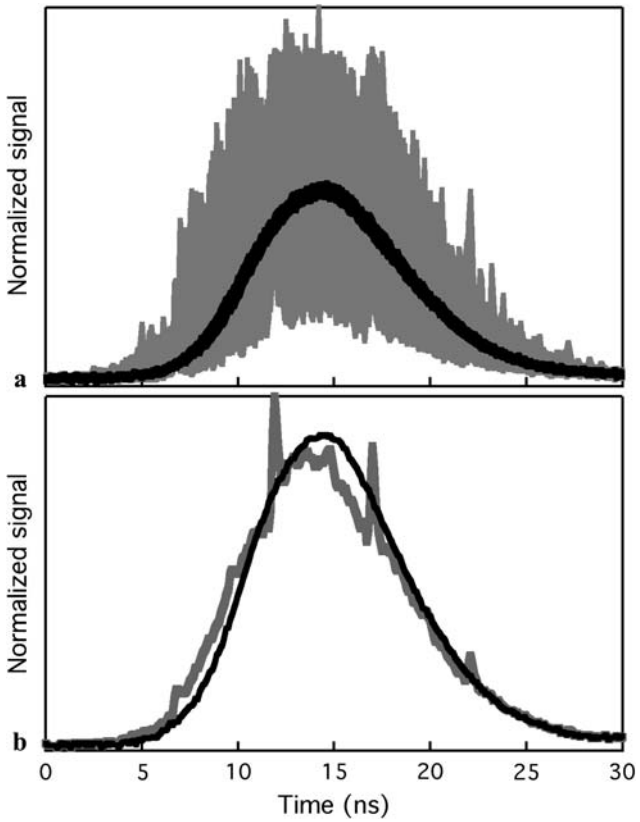

Fig. 2 Laser temporal profiles of (**a**) 300 single laser pulses and (**b**) an average of 300 laser pulses with the laser seeded (*black lines*) and not seeded (*grey lines*). The traces have been normalized such that the areas under the curves are the same

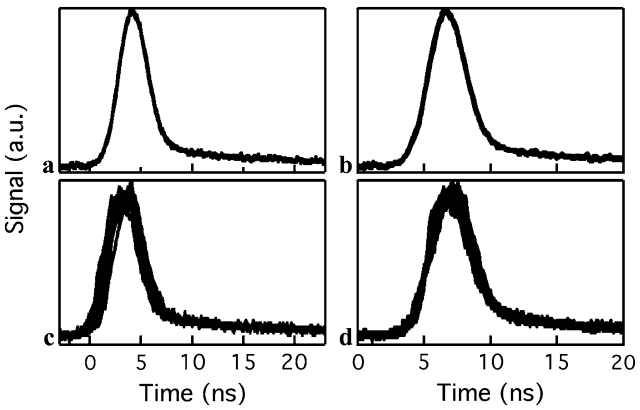

Fig. 3 Twenty single-pulse LII temporal profiles recorded at a fluence of 0.6 J/cm^2 with the laser seeder (**a**) and (**b**) turned on and (**c**) and (**d**) turned off. LII profiles in (**b**) and (**d**) are shifted to match the median of the corresponding laser profile at 10 ns

with the unseeded laser (Fig. 3c) show a significant spread of the LII signal rising edge. This spread is due to the sensitivity of the soot response to the laser intensity fluctuations as well as to the time jitter in the optical trigger of the LII acquisition attributable to the variability in the timing of the mode structure on the laser temporal profile. To account

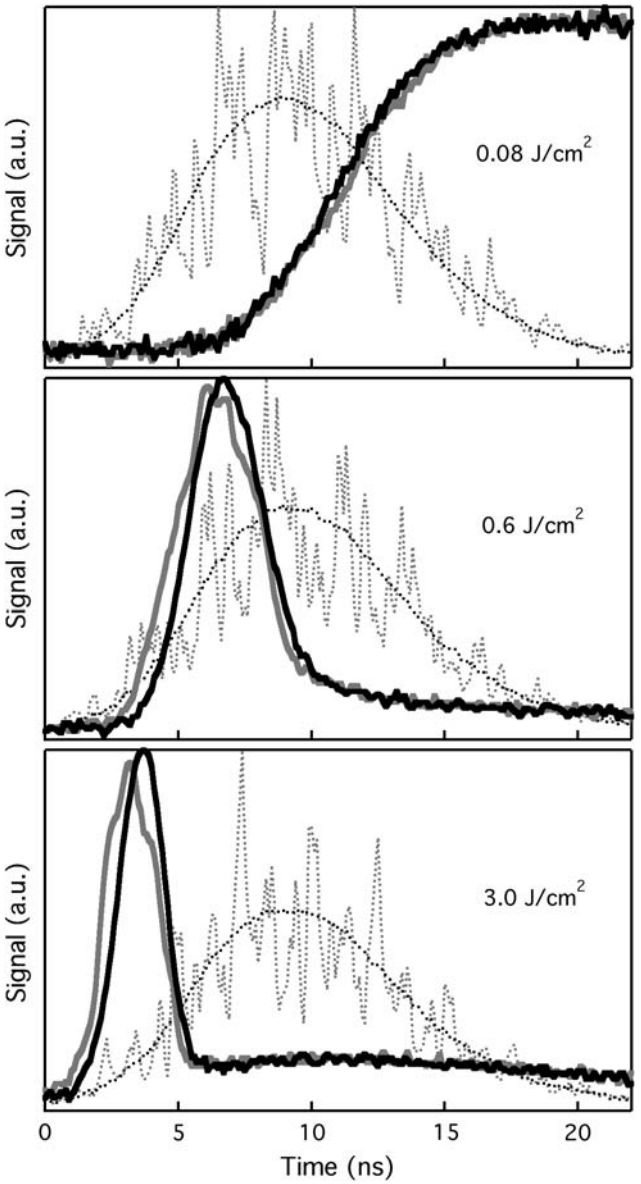

Fig. 4 Single-pulse LII temporal profiles recorded with the laser seeder turned on (*black lines*) and off (*grey lines*) at different laser fluences. The corresponding laser profiles (*dotted lines*) are also displayed. The LII temporal profiles are shifted to match the median of the corresponding laser profile at 10 ns

for that jitter, in Figs. 3b and d the LII profiles have been shifted to match the median of the corresponding laser pulse at 10 ns. In the case of the unseeded laser the shifting procedure reduces the dispersion of the LII signal leading edge. In Fig. 3d there is still a noticeable spread due to the effect of laser intensity fluctuations on the soot LII response.

Figure 4 shows representative single-pulse LII temporal profiles recorded with the seeder on (black lines) and with the seeder off (grey lines). The dotted lines show the corresponding laser profiles. Data shown were taken at fluences of 0.08, 0.6, and 3.0 J/cm^2. The laser and the LII profiles

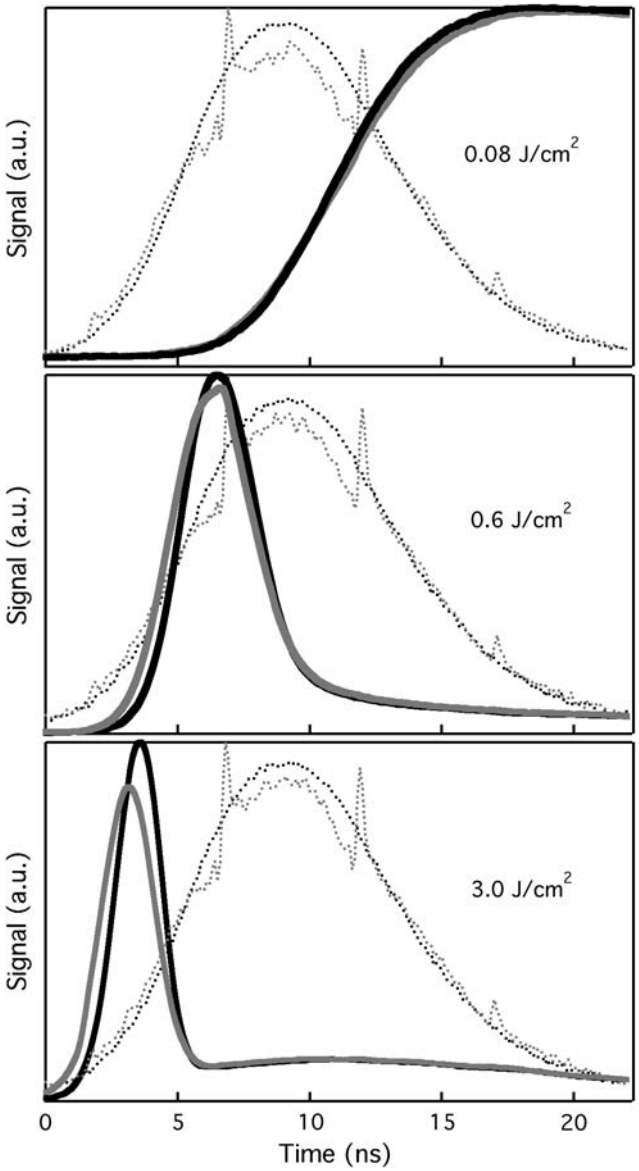

Fig. 5 LII temporal profiles averaged for 300 laser pulses recorded with the seeder turned on (*black lines*) and off (*grey lines*) at different laser fluences. The corresponding laser profiles (*dotted lines*) are also displayed. The LII temporal profiles are shifted to match the median of the corresponding laser profile at 10 ns

in Fig. 4 are shifted to match the median of the laser profile at 10 ns. At low fluence (0.08 J/cm^2), although the two single-pulse laser profiles displayed in Fig. 4 differ significantly, the LII temporal profiles recorded with the seeder on and the seeder off are similar. At this fluence the LII signal rise time due to the soot laser heating and the LII signal decay time due to the conductive cooling of the particles are much longer than the characteristic time of the unseeded laser intensity fluctuations. The unseeded laser intensity fluctuations therefore have a negligible effect on the single-pulse rise time of the LII signal. Figure 5 shows averages of 300 shots of the unseeded and seeded laser temporal

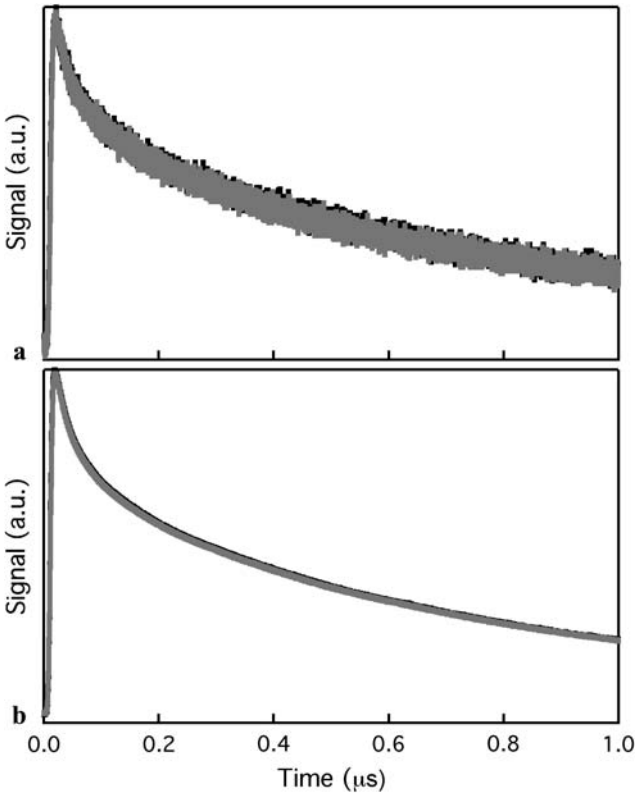

Fig. 6 Single-pulse (**a**) and averaged (**b**) LII temporal profiles at long delay time recorded with the seeder turned on (*black lines*) and off (*grey lines*) at a fluence of 0.08 J/cm^2

profiles and corresponding LII signals at the same fluences as displayed in Fig. 4. As with the single-pulse data, at the lowest fluence the LII rise time is insensitive to whether the laser is seeded. Figure 6 shows (a) single-pulse and (b) averaged LII temporal profiles recorded at long delay time at a fluence 0.08 J/cm^2 with the seeder on (black lines) and off (grey lines). The mode structure in the temporal profiles of the unseeded laser pulses does not affect the measured decay rate of either the single-pulse or the averaged data, and hence primary particle size inferred from the data at this low fluence will be insensitive to whether the laser is seeded.

As seen in Fig. 4, the characteristic time for heating the soot particles decreases with increasing laser fluence and at intermediate fluences becomes on the order of the characteristic time of the mode structure in the temporal profile of the unseeded laser pulses. At fluences higher than 0.2 J/cm^2 graphite sublimation and fast non-thermal photodesorption of carbon clusters strongly contribute to the reduction of the particle size by formation of mainly C_3 and C_2 clusters [22]. This rapid reduction in particle size precipitates a fast LII signal decay [34]. Fast LII signal rise times and decay rates lead to LII temporal profiles that are highly dependent on the laser intensity fluctuations. At 0.6 and 3.0 J/cm^2 the single-pulse LII signal rises earlier in the case of the unseeded laser than for the seeded laser because of high-intensity peaks at

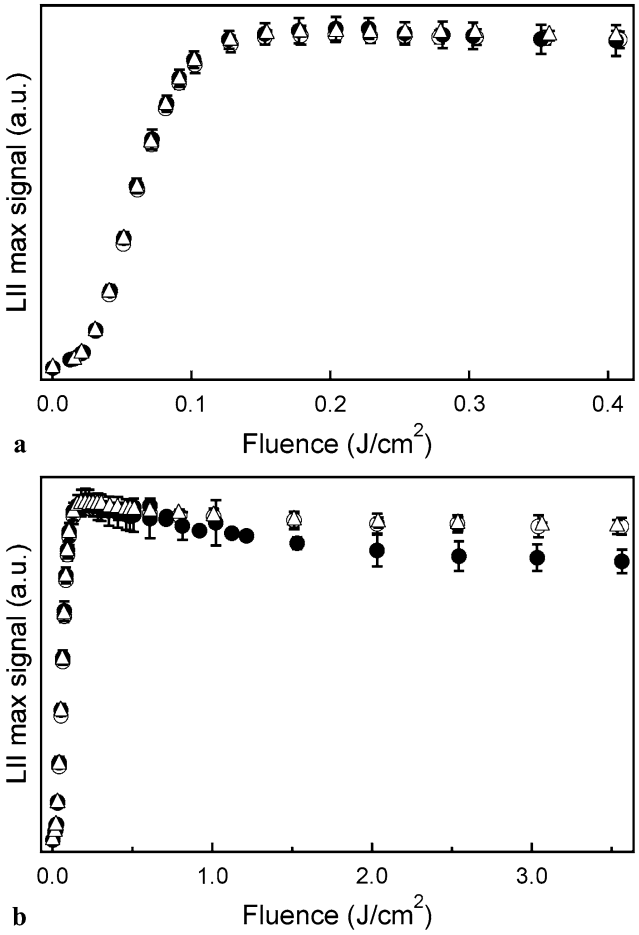

Fig. 7 Fluence dependence of the peak of the averaged LII temporal profile at (**a**) low and intermediate fluences and (**b**) over the full experimental fluence range. Each temporal profile is from the average of 300 laser pulses. Data are shown for optically triggered signals using a laser running either seeded (*open circles*) or unseeded (*closed circles*). Data are also shown for signals collected using the laser Q-switch to trigger the LII acquisition (*open triangles*) using a seeded laser. Error bars represent $2-\sigma$ standard deviation of the mean of at least nine sets of 300 shot averages

the leading edge of the laser profile, as shown in Fig. 4. At these high fluences structure in the single-pulse LII temporal profiles is also observable at the position of the maximum signal intensity.

At intermediate and high fluences, as shown in Fig. 5, although the average of the unseeded laser pulse shows a relatively smooth profile, the corresponding averaged LII temporal profile is different from the one recorded for the seeded laser. Any high-intensity laser peaks on the leading edge of the single-pulse laser profiles cause the averaged LII signal from the unseeded laser pulse to rise faster than the corresponding profiles for the seeded laser. Therefore, averaging the LII profiles from an unseeded laser leads to a temporal profile that is broader than that recorded using a seeded laser pulse. The temporal maximum intensity of the LII signal is also lower when an unseeded laser is used.

LII temporal maximum Figure 7 shows the LII temporal maximum for the data recorded with the seeder turned on and turned off. The fluence curves are the average of at least nine independent datasets (each an average of 300 shots), and error bars are given as the two-sigma standard deviation of the mean. At fluences below 0.3 J/cm^2 (see Fig. 7a) the LII temporal maximum is similar for all the laser configurations considered. At these low fluences, as discussed above, the particle heating and cooling rates are much slower than the laser intensity fluctuations. The fluence dependence of the LII temporal maximum is therefore insensitive to whether the laser is seeded. At fluences from 0.3 to 0.6 J/cm^2 the LII temporal maximum using the unseeded laser appears to be lower than the temporal maximum using the seeded laser, but the differences are statistically insignificant. At fluences higher than 0.6 J/cm^2 the differences are more significant. In the case of the unseeded laser the averaged LII temporal maximum decreases by up to 10% with increasing fluence, whereas it is almost independent of fluence for the seeded laser. The pulse-to-pulse variability in the timing of the mode structure of the unseeded laser greatly affects the average LII temporal maximum at fluences above ~0.6 J/cm^2, for which the LII signal rise and decay are on the order of the laser fluctuations.

For both laser configurations a prompt gated signal was simulated by integrating the LII temporal profile over a 20-ns time interval centered on the laser pulse. The broader LII temporal profile combined with the lower temporal maximum obtained when using an unseeded laser lead to an integrated LII signal that is within 5% of the corresponding integrated seeded-LII signal. The fast laser intensity fluctuations therefore are not expected to significantly affect the soot volume fraction inferred from the gated LII signal.

3.2 Influence of data acquisition triggering schemes

In order to study the effect of the trigger jitter on the LII averaged profiles, we have collected and compared averaged data using (1) a fast photodiode measuring the laser output, (2) the Q-switch, and (3) the modified flashlamp synchronization pulse to trigger the data acquisition. The flashlamp pulse was modified using a low-pass electrical filter that effectively increases the rise time of the leading edge of the pulse. The data acquisition jitter was characterized by recording 300 single seeded-laser pulses and comparing the timing of the laser maximum intensity to that of the average profile. Figure 8 shows distributions of time differences for 300 pulses relative to the mean for each triggering scheme. Gaussian fits to the distributions yield values for the width (FWHM) of 0.11 ns using the photodiode signal, 0.63 ns using the Q-switch pulse, and 1.19 ns using the modified flashlamp synchronization pulse. The jitter recorded using the photodiode signal is the measure of jitter between the

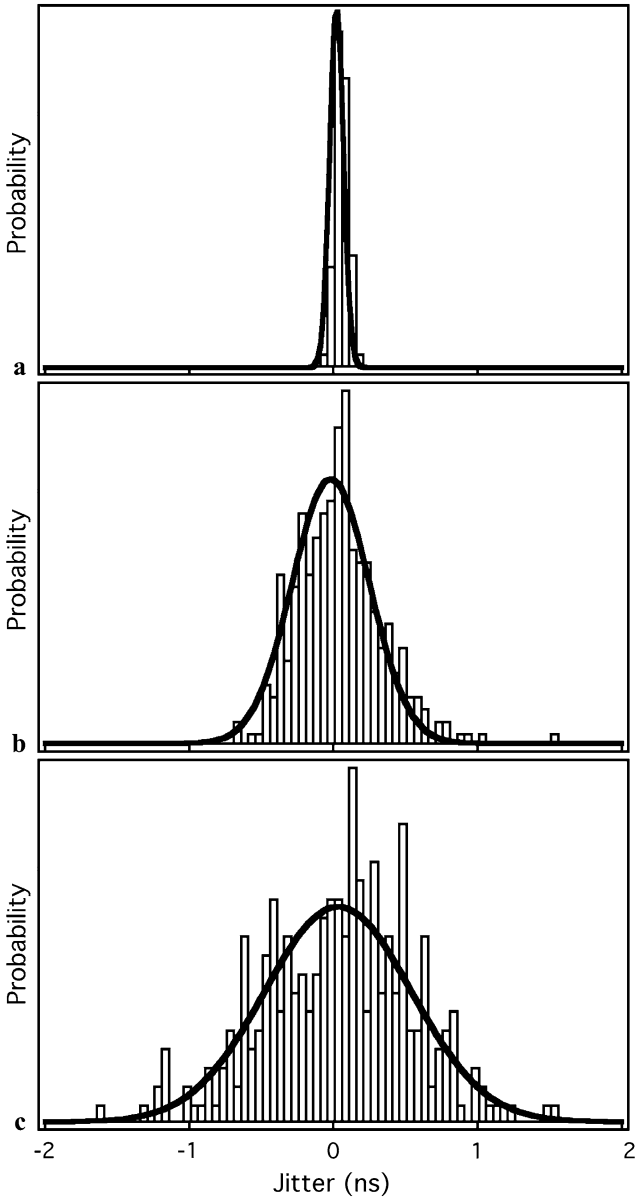

Fig. 8 Time jitter distribution recorded for 300 single-pulse seeded-laser profiles when triggering the data acquisition using (**a**) optical triggering, (**b**) the laser Q-switch, and (**c**) the low-pass-filtered flashlamp synchronization pulse. The *solid lines* are the fit to the data using a Gaussian distribution, giving a FWHM of (**a**) 0.11, (**b**) 0.63, and (**c**) 1.19 ns

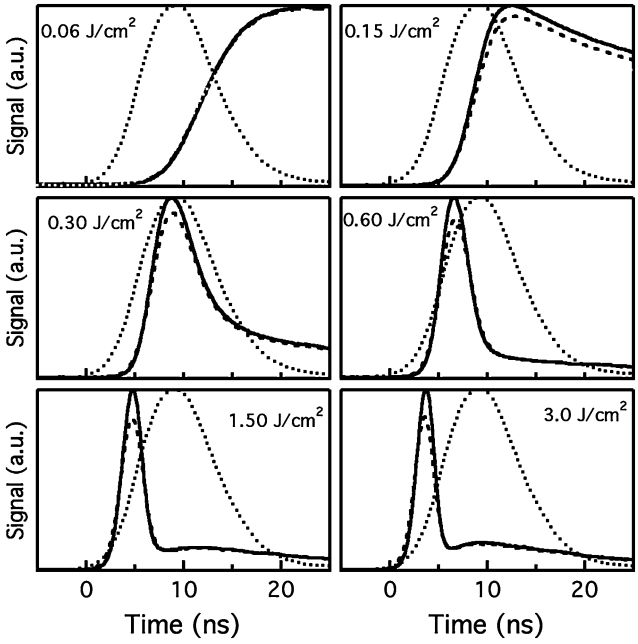

Fig. 9 Effect of trigger jitter on LII temporal profiles. LII temporal profiles averaged for 300 laser pulses are shown using the laser Q-switch (*solid lines*) and the low-pass-filtered flashlamp synchronization pulse (*dashed lines*) to trigger the data acquisition. The profiles recorded with the Q-switch pulse trigger are identical to those recorded using the optical trigger. The *dotted lines* are the laser profiles for the optical trigger

1064-nm output of the laser and the 532-nm output recorded on different channels of the oscilloscope and represents the time resolution of the photodiodes used. The timing jitter measured between the Q-switch and the optical output is nearly within the specifications of our laser (<0.5 ns). Figure 7 shows the maximum of averaged LII temporal profiles using the Q-switch and modified flashlamp synchronization pulses to trigger the experiment compared with data taken with the optical trigger. This figure demonstrates that using the Q-switch with a jitter of 0.63 ns (FWHM) to trigger the experiment does not affect the normalized average LII temporal maximum. Some lasers may have more time variability between the firing of the Q-switch and the output pulse, which is why we have repeated the experiment using the modified flashlamp synchronization pulse.

Figure 9 displays the averaged LII temporal profiles recorded using the laser Q-switch (solid lines) and the low-pass-filtered flashlamp synchronization pulse (dashed lines) to trigger the data acquisition. The dotted line represents the laser profile in the case of the optical trigger. The corresponding profiles using the optical trigger are identical to those using the Q-switch trigger. At low fluence the rise time and decay time of the LII response are slow enough that the additional jitter does not significantly affect the averaged LII temporal profiles. At fluences of 0.15 J/cm^2 and higher the average profiles recorded using the flashlamp pulse are significantly lower (up to 15%) than those recorded using the optical trigger and laser Q-switch pulse. The fast rise time and decay rate of the LII signal and the sharp LII peak are not captured with the flashlamp-pulse trigger because of the degradation of the temporal resolution introduced by the trigger jitter.

The prompt gated signal, simulated by integrating the flashlamp-triggered LII temporal profile over a 20-ns time interval centered on the laser pulse, differs by less than 10% from the corresponding simulated gated signal obtained with

a time jitter smaller than 1 ns. Soot volume fractions inferred from gated LII are therefore not expected to be significantly affected by a time jitter shorter than 1.2 ns.

4 Conclusions

Single laser pulse and averaged LII temporal profiles have been recorded with a sub-nanosecond time resolution over a wide range of fluences using unseeded and seeded laser pulses. At fluences below ∼0.3 J/cm^2 the LII rise and decay times are much longer than the characteristic time of the intensity fluctuations on the unseeded laser temporal profile. The LII signal is not significantly affected by the laser intensity fluctuations caused by mode structure on the unseeded laser pulses. At higher fluences the rise time and decay time of the LII signal are on the order of the characteristic time of these laser intensity fluctuations, and the averaged temporal profiles recorded using the unseeded laser are broader and appear earlier in time than those recorded using the seeded laser. At fluences below 0.6 J/cm^2 the effect of the unseeded laser mode structure on the LII temporal maximum is within the experimental uncertainties. At higher fluences, the unseeded laser temporal mode structure greatly affects the shape of the single-shot and averaged LII temporal profiles and the fluence dependence of the averaged LII temporal maximum.

Averaged LII temporal profiles recorded using the laser Q-switch (∼0.63-ns jitter) to trigger the data acquisition show a negligible effect of the jitter on averaged LII profiles up to a fluence of 3.5 J/cm^2. Using the low-pass-filtered flashlamp synchronization pulse (∼1.19-ns jitter) to trigger the experiment, however, makes the averaged LII temporal profile broader and reduces the LII temporal maximum for fluences as low as 0.15 J/cm^2. For measurements of either time-resolved or gated LII signals, care should be taken to assess the timing jitter between the trigger chosen and the optical output of the laser. Reducing or eliminating the timing jitter is particularly important at intermediate and high laser fluences.

LII signals obtained with either an unseeded laser or a trigger with 1.2-ns jitter and integrated over a 20-ns time interval centered on the laser pulse do not differ by more that 10% from the corresponding integrated signal obtained using a seeded laser pulse with optical triggering. Thus, neither fast laser temporal fluctuations nor trigger jitter are expected to have a significant effect on soot volume fraction inferred from prompt gated LII.

The present study, however, highlights some difficulties in measuring reliable LII temporal profiles for validating LII models. Fluence fluctuations in the unseeded laser temporal profile can lead to significant perturbations to the LII temporal profiles at fluences as low as 0.15 J/cm^2. A time jitter of 1.2 ns in the data acquisition trigger will significantly decrease the temporal maximum at fluences as low as 0.15 J/cm^2. These perturbations limit the usefulness of these LII temporal profiles for LII model validation at these fluences.

Acknowledgements This work was supported by the Division of Chemical Sciences, Geosciences, and Biosciences, the Office of Basic Energy Sciences, the US Department of Energy. Sandia is a multiprogram laboratory operated by Sandia Corporation, a Lockheed Martin Company, for the National Nuclear Security Administration under contract DE-AC04-94-AL85000.

References

1. R.J. Santoro, C.R. Shaddix, Laser-induced incandescence, in *Applied Combustion Diagnostics*, ed. by K. Kohse-Höinghaus, J.B. Jeffries (Taylor & Francis, London, 2002), p. 252
2. L.A. Melton, Appl. Opt. **23**, 2201 (1984)
3. D.L. Hofeldt, Soc. Automot. Eng. Tech. Pap. Ser. **102**(4), 45 (1993)
4. N.P. Tait, D.A. Greenhalgh, Ber. Bunsenges. Phys. Chem. **97**, 1619 (1993)
5. R.W. Weeks, W.W. Duley, J. Appl. Phys. **45**, 4661 (1974)
6. S. Will, S. Schraml, A. Leipertz, Opt. Lett. **20**, 2342 (1995)
7. P. Roth, A.V. Filippov, J. Aerosol Sci. **27**, 95 (1996)
8. B. Mewes, J.M. Seitzman, Appl. Opt. **36**, 709 (1997)
9. S. Will, S. Schraml, K. Bader, A. Leipertz, Appl. Opt. **37**, 5647 (1998)
10. B. Axelsson, R. Collin, P.-E. Bengtsson, Appl. Opt. **39**, 3683 (2000)
11. C. Allouis, F. Beretta, A. D'Alessio, Exp. Therm. Fluid Sci. **27**, 455 (2003)
12. T. Schittkowski, B. Mewes, D. Brüggemann, Phys. Chem. Chem. Phys. **4**, 2063 (2002)
13. R. Starke, P. Roth, Combust. Flame **127**, 2278 (2002)
14. T. Lehre, B. Jungfleisch, R. Suntz, H. Bockhorn, Appl. Opt. **42**, 2021 (2003)
15. V. Krüger, C. Wahl, R. Hadef, K.P. Geigle, W. Stricker, M. Aigner, Meas. Sci. Technol. **16**, 1477 (2005)
16. M. Hofmann, W.G. Bessler, C. Schulz, H. Jander, Appl. Opt. **42**, 2052 (2003)
17. K.A. Thomson, D.R. Snelling, G.J. Smallwood, F. Liu, Appl. Phys. B **83**, 469 (2006)
18. M. Hofmann, F. Kock, T. Dreier, H. Jander, C. Schulz, Appl. Phys. B **90**, 629 (2008)
19. G.B. Kim, J.Y. Shim, S.W. Cho, Y.J. Chang, C.H. Jeon, J. Mech. Sci. Technol. **22**, 1154 (2008)
20. P. Desgroux, X. Mercier, B. Lefort, R. Lemaire, E. Therssen, J.F. Pauwels, Combust. Flame **155**, 289 (2008)
21. R.L. Vander Wal, K.J. Weiland, Appl. Phys. B **59**, 445 (1994)
22. F. Goulay, P.E. Schrader, L. Nemes, M.A. Dansson, H.A. Michelsen, Proc. Combust. Inst. **32**, 963 (2009)
23. T. Ni, J.A. Pinson, S. Gupta, R.J. Santoro, Appl. Opt. **34**, 7083 (1995)
24. D. Snelling, F. Liu, G.J. Smallwood, Ö.L. Gülder, in *Proc. 34th Natl. Heat Transfer Conf.* (NHTC2000) (2000)
25. H.A. Michelsen, P.O. Witze, D. Kayes, S. Hochgreb, Appl. Opt. **42**, 5577 (2003)
26. H. Bladh, P.-E. Bengtsson, Appl. Phys. B **78**, 241 (2004)
27. J. Delhay, Y. Bouvier, E. Therssen, J.D. Black, P. Desgroux, Appl. Phys. B **81**, 181 (2005)
28. M.A. Dansson, M. Boisselle, M.A. Linne, H.A. Michelsen, Appl. Opt. **46**, 8095 (2007)

29. H.A. Michelsen, Appl. Phys. B **83**, 443 (2006)
30. J. Appel, B. Jungfleisch, M. Marquardt, R. Suntz, H. Bockhorn, Proc. Combust. Inst. **26**, 2387 (1996)
31. R.L. Vander Wal, Appl. Opt. **35**, 6548 (1996)
32. R.L. Vander Wal, T.M. Ticich, A.B. Stephens, Appl. Phys. B **67**, 115 (1998)
33. P.O. Witze, S. Hochgreb, D. Kayes, H.A. Michelsen, C.R. Shaddix, Appl. Opt. **40**, 2443 (2001)
34. H.A. Michelsen, J. Chem. Phys. **118**, 7012 (2003)
35. S. De Iuliis, F. Migliorini, F. Cignoli, G. Zizak, Appl. Phys. B **83**, 397 (2006)
36. C. Schulz, B.F. Kock, M. Hofmann, H.A. Michelsen, S. Will, B. Bougie, R. Suntz, G.J. Smallwood, Appl. Phys. B Lasers Opt. **83**, 333 (2006)
37. R.L. Vander Wal, K.A. Jensen, Appl. Opt. **37**, 1607 (1998)
38. D.R. Snelling, F. Liu, G.J. Smallwood, Ö.L. Gülder, Combust. Flame **136**, 180 (2004)
39. A.C. Eckbreth, J. Appl. Phys. **48**, 4473 (1977)
40. A.V. Filippov, M.W. Markus, P. Roth, J. Aerosol Sci. **30**, 71 (1999)
41. F. Liu, G.J. Smallwood, D.R. Snelling, J. Quant. Spectrosc. Radiat. Transfer **93**, 301 (2005)
42. R.J. Santoro, H.G. Semerjian, R.A. Dobbins, Combust. Flame **51**, 203 (1983)
43. R.J. Santoro, J.H. Miller, Langmuir **3**, 244 (1987)
44. R.A. Dobbins, C.M. Megaridis, Langmuir **3**, 254 (1987)
45. Ü.Ö. Köylü, C.S. McEnally, D.E. Rosner, L.D. Pfefferle, Combust. Flame **110**, 494 (1997)
46. R.A. Fletcher, R.A. Dobbins, H.-C. Chang, Anal. Chem. **70**, 2745 (1998)
47. K. Lee, Y. Han, W. Lee, J. Chung, C. Lee, Meas. Sci. Technol. **16**, 519 (2005)
48. K.C. Smyth, C.R. Shaddix, D.A. Everest, Combust. Flame **111**, 185 (1997)